Cancer Research

Neutralization of Tumor Acidity Improves Antitumor Responses to Immunotherapy

Shari Pilon-Thomas[1], Krithika N. Kodumudi[1], Asmaa E. El-Kenawi[2,3], Shonagh Russell[2], Amy M. Weber[1], Kimberly Luddy[2], Mehdi Damaghi[2], Jonathan W. Wojtkowiak[2], James J. Mulé[1], Arig Ibrahim-Hashim[2], and Robert J. Gillies[2]

Abstract

Cancer immunotherapies, such as immune checkpoint blockade or adoptive T-cell transfer, can lead to durable responses in the clinic, but response rates remain low due to undefined suppression mechanisms. Solid tumors are characterized by a highly acidic microenvironment that might blunt the effectiveness of antitumor immunity. In this study, we directly investigated the effects of tumor acidity on the efficacy of immunotherapy. An acidic pH environment blocked T-cell activation and limited glycolysis *in vitro*. IFNγ release blocked by acidic pH did not occur at the level of steady-state mRNA, implying that the effect of acidity was posttranslational. Acidification did not affect cytoplasmic pH, suggesting that signals transduced by external acidity were likely mediated by specific acid-sensing receptors, four of which are expressed by T cells. Notably, neutralizing tumor acidity with bicarbonate monotherapy impaired the growth of some cancer types in mice where it was associated with increased T-cell infiltration. Furthermore, combining bicarbonate therapy with anti-CTLA-4, anti-PD1, or adoptive T-cell transfer improved antitumor responses in multiple models, including cures in some subjects. Overall, our findings show how raising intratumoral pH through oral buffers therapy can improve responses to immunotherapy, with the potential for immediate clinical translation. *Cancer Res; 76(6); 1381–90. ©2015 AACR.*

Introduction

The amplitude and quality of T-cell activation in response to antigen activation of the T-cell receptor (TCR) is tightly controlled by the engagement of inhibitory receptors, such as PD-1, Lag-3, Tim-3, BTLA, and CTLA4. The ability of tumors to coopt these inhibitory pathways plays an important role in the inhibition of T-cell responses within the tumor microenvironment (1, 2). Treatment with fully humanized neutralizing mAbs against CTLA4, PD-1, or its ligand PD-L1 has led to durable antitumor responses where conventional therapies have failed (3–5). However, response rates remain low, from 18% to 27% for anti-PD-1 antibodies (6) and 11% for anti-CTLA4 antibodies (7). Recent studies have shown that multiple checkpoints can be coexpressed on individual tumor–infiltrating lymphocytes, such as PD-1$^+$TIM-3$^+$ T cells, which are defective in proliferation and cytokine production (8–10). Indeed, a recent clinical trial combined PD-1 and CTLA4 blockade in patients with melanoma and showed an increase rate of objective tumor responses as compared with blocking either checkpoint alone, 40% versus 20% (11). However, there remain a significant proportion of nonresponders, suggesting that additional immunosuppressive pathways are active.

Regulatory T cells (Treg) or myeloid-derived suppressor cells (MDSC) are also known to blunt T-cell responses (12, 13). Tregs suppress antigen-specific T-cell response, and the removal of Tregs in murine models led to enhanced antitumor T-cell responses and tumor rejection (14). MDSCs are comprised of immature macrophages, granulocytes, and dendritic cells (DC; ref. 15). They suppress T-cell responses, reduce antigen-specific CD8$^+$ T-cell proliferation, and increase T-cell death by apoptosis (16), and their elimination has been shown to enhance antitumor immunity and tumor regression in murine tumor models (17). In addition to these cell-based inhibitors of immune function, there are also secreted factors that block T-cell activation. The most widely studied of these are the kynurenines, which are synthesized by the tryptophan-metabolizing enzyme, indoleamine-2,3-dioxygenase (IDO). IDO can be expressed by cancer cells and is normally expressed by DCs in response to IFNγ to blunt immune activation (18). There has also been evidence that tumor-derived acidity also plays a role in immunosuppression (19).

Solid tumors are unequivocally acidic (20). This is commonly believed to be a consequence of high rates of fermentative metabolism in a poorly perfused environment (21). However, newer models point to an active role for the membrane-bound carbonic anhydrase IX (CAIX) in establishing extracellular acidity (22). This is relevant, as CAIX is an independent negative prognostic indicator in a number of cancers, including, *inter alia*, breast (23), lung (24), and ovarian cancers (25).

[1]Department of Immunology, H. Lee Moffitt Cancer Center and Research Institute, Tampa, Florida. [2]Department of Cancer Imaging and Metabolism, H. Lee Moffitt Cancer Center and Research Institute, Tampa, Florida. [3]Department of Pharmacology and Toxicology, Faculty of Pharmacy, Mansoura University, Mansoura, Egypt.

Note: Supplementary data for this article are available at Cancer Research Online (http://cancerres.aacrjournals.org/).

Corresponding Author: Robert J. Gillies, Moffitt Cancer Center and Research Institute, 12901 Magnolia Dr, SRB 24000E, Tampa, FL 33612. Phone: 813-745-8355; Fax: 813-979-7265; E-mail: Robert.Gillies@moffitt.org

doi: 10.1158/0008-5472.CAN-15-1743

Tumor acidity is important to tumor progression, as it has been shown to promote local invasion and metastasis (26), and metastasis can be inhibited by neutralization of acidity with oral buffers (27, 28).

Tumor-derived acidity is also hypothesized to suppress immune function (19). For example, lactic acidosis is a strong negative prognostic indicator in sepsis (29). *In vitro*, acidic pH (6.5) can suppress T-cell functions, including IL2 secretion and the activation of T-cell receptors (30), although the mechanism by which this occurs is not known. Likewise, there is evidence that acid pH affects other components of the immune system, such as DCs, MDSCs, or macrophages, yet these effects are also not known with certainty (19). For example, inhibition of proton pumps on tumor cells with omeprazole can hamper tumor-induced suppression of macrophages *in vitro* and *in vivo* (31, 32), yet this activity may be due to off-target effects, as the target for these drugs are not known to be expressed in the immune system. It may be assumed that the effects of acidity are not mediated via acidification of the intracellular pH (pHi), as the pHi has been shown to be highly buffered in activated T cells (33). More recently, families of specific acid–sensing receptors have been identified (34) and shown to transduce extracellular acidity into intracellular signals. For example, acid pH has been shown to activate the G-protein, T-cell inhibitory receptor, T-cell death–associated gene-8 (*TDAG8*; ref. 35), and this has been shown to be responsible for a reduction in c-myc translation in lymphocytes (36). In this study, we examined the effect of tumor acidity on antitumor immunotherapeutic strategies and observed that the neutralization of tumor pH with bicarbonate increased response to checkpoint inhibitors and, importantly, led to cures in combination with adoptive T-cell therapy.

Materials and Methods

Mice

Female C57BL/6 mice (6–8 weeks old) were purchased from Harlan Laboratories. TDAG8 knockout (TDAG8 KO) mice on the C57BL/6 background were purchased from The Jackson Laboratory. Pmel, OT-I, and OT-II mice were bred and housed at the Animal Research Facility of the H. Lee Moffitt Cancer Center and Research Institute (Tampa, FL). Mice were humanely euthanized by CO_2 inhalation according to the American Veterinary Medical Association Guidelines. Mice were observed daily and were humanely euthanized if a solitary subcutaneous tumor exceeded 200 cm^2 in area or mice showed signs referable to metastatic cancer. All animal experiments were approved by the Institutional Animal Care and Use Committee and performed in accordance with the U.S. Public Health Service Policy and National Research Council Guidelines.

Cell lines and cell culture

B16 melanoma (obtained from ATCC), Yumm 1.1 melanoma (kindly provided by Marcus Bosenberg, Yale University, New Haven, CT), and Panc02 pancreatic cancer (a kind gift from Emmanual Zervos, East Carolina University, Greenville, NC) cell lines were cultured in complete media (CM): RPMI media supplemented with 10% heat-inactivated FBS, 0.1 mmol/L nonessential amino acids, 1 mmol/L sodium pyruvate, 2 mmol/L fresh L-glutamine, 100 mg/mL streptomycin, 100 U/mL penicillin, 50 mg/mL gentamicin, 0.5 mg/mL fungizone (all from Life Technologies), and 0.05 mmol/L 2-ME (Sigma-Aldrich). The cell lines tested negative for mycoplasma contamination. All cell lines were passaged less than 10 times after initial revival from frozen stocks. All cell lines were validated in core facilities prior to use.

In vitro T-cell culture

T cells were isolated from the spleens of pmel, OT-I, or OT-II mice using T-cell columns (R&D Systems). Pmel T cells were cultured for 2 days in CM, containing 10 IU/mL IL2 and 5 μg/mL $gp100_{25\text{-}33}$ peptide. T cells were collected and cultured in CM, pH 6.6 or 7.4, with $gp100_{25\text{-}33}$ peptide (10 mcg/mL) for 24 hours. Freshly isolated OT-I T cells were cultured in CM, pH 6.6 or 7.4, with $OVA_{SIINFEKL}$ peptide (10 mcg/mL) for 24 hours. Freshly isolated OT-II T cells were cultured in CM, pH 6.6 or 7.4, with $OVA_{323\text{-}339}$ peptide (10 mcg/mL) for 24 hours. Freshly isolated T cell from TDAG8 KO and wild-type (WT) littermates were cultured with 5 mcg/mL plate-bound anti-CD3 antibodies for 48 hours. For restimulation experiments, pmel T cells were collected after 24 hours of culture in CM, pH 6.6 or pH 7.4, containing 10 mcg/mL $gp100_{25\text{-}33}$ peptide and recultured in CM, pH 7.4, with 10 mcg/mL $gp100_{25\text{-}33}$ peptide for 24 to 48 hours. Cell supernatants were collected and IFNγ production was measured by ELISA. For measurement of IFNγ production by flow cytometry, brefeldin A (1 mcg/mL) was added to the cell culture 4 hours prior to harvest. Cells were harvested and stained with live/dead Aqua (Invitrogen) to exclude dead cells. Surface staining was done with anti-mouse CD8 APC antibody, followed by intracellular staining with anti-mouse IFNγ PE, and data were acquired on the LSR II and analyzed using FlowJo software.

Treatment model

C57BL/6 mice received 200 mmol/L of sodium bicarbonate water 3 days prior to tumor injection and continued to receive bicarbonate water until the end of the experiment. Control mice received regular tap water. A total of 1×10^5 B16, Yumm 1.1, or Panc02 tumor cells were injected subcutaneously in the left flank of C57BL/6 mice. Mice received intraperitoneal injections of 20 mg/kg of anti-PD1 or anti-CTLA4 antibodies on day 3 and continued to receive antibodies every 3 to 4 days until the end of the experiment. Mice were humanely euthanized when tumors exceeded 1.5 cm in diameter, appeared necrotic, or interfered with locomotion. Tumors were collected and weighed.

Adoptive T-cell therapy

C57BL/6 mice received 200 mmol/L of sodium bicarbonate water 3 days prior to tumor injection and continued to receive bicarbonate water until the end of the experiment. Control mice received regular tap water. A total of 1×10^5 B16 tumor cells were injected subcutaneously in the left flank of C57BL/6 mice. Three days later, mice received a sublethal dose (600 cGy) of total body irradiation (TBI) administered by an X-ray irradiator. For adoptive transfer experiments, T cells were isolated from the spleens of pmel mice and cultured in media containing 10 IU/mL of IL2 and 5 μg/mL of $gp100_{25\text{-}33}$ *in vitro* for 5 days. On day 4 following tumor injection, 5×10^6 T cells were intravenously injected. IL2 (2.5e5 IU) was given intraperitoneally following T-cell injection, continuing every 12 hours for 3 days, for a total of 6 injections. Following this treatment, tumor size was measured and recorded every 2 days.

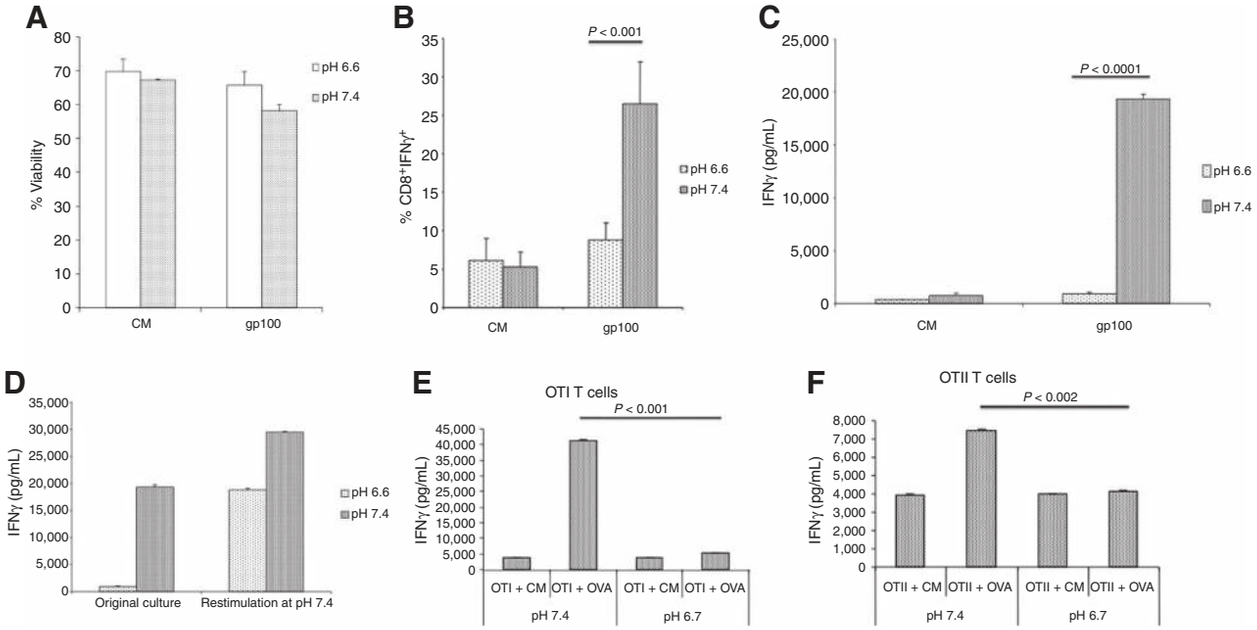

Figure 1.

Effect of pH on activation of T cells. T cells were activated at pH 7.4 for 48 hours with either $gp100_{25\text{-}33}$ peptide (pmel T cells; A–D) or $OVA_{SIINFEKL}$ peptide (OT-1 or OT-2 T cells; E–F) or left unactivated in CM, followed by an incubation at either pH 6.6 or 7.4 for additional 24 hours. A, percent cell viability of $CD8^+$ pmel T cells following the entire treatment as measured by flow cytometry. B, percentage of $CD8^+$ pmel T cells that contained IFNγ as measured by flow cytometry. C, amount of IFNγ secreted into the media by pmel T cells as measured by ELISA following the second 24-hour incubation at pH 6.6 or 7.4. D, IFNγ production by pmel T cells after replating from pH 6.6 to 7.4 as measured by ELISA. Activated pmel T cells were cultured in CM for 24 hours at pH 6.6 or 7.4 (original culture). After 24 hours, cells were collected and replated at pH 7.4 with gp100 peptide (restimulation at pH 7.4). Culture supernatants were collected after 24 hours for IFNγ measurement by ELISA. E, IFNγ secreted into the media by $CD8^+$ OT-1 T cells measured by ELISA following second 24-hour incubation at pH 6.7 or 7.4. F, amount of IFNγ secreted into the media by $CD4^+$ OT-II T cells measured by ELISA following the 2nd 24-hour incubation at pH 6.7 or 7.4. Data, mean ± SD from a minimum of three independent experiments. *P* values were determined by two-tailed Student *t* test.

Flow cytometry

Spleens and tumors were harvested under sterile conditions. Single-cell suspensions were prepared, and red blood cells were removed using ACK lysis buffer. Tumor cell suspensions were prepared from solid tumors by enzymatic digestion in Hank's Balanced Salt Solution (HBSS) (Life Technologies), containing 1 mg/mL collagenase, 0.1 mg/mL DNAse I, and 2.5 U/mL of hyaluronidase (all from Sigma-Aldrich), with constant stirring for 2 hours at room temperature. The resulting suspension was passed through a 70-μm cell strainer and washed once with HBSS. Cells were resuspended in PBS + 3% BSA to a concentration of 0.5–1 × 10^6 cells/mL for flow cytometric analysis. After red blood cell lysis with ACK buffer, cells were stained in FACS buffer with the following antibodies for flow cytometric analysis: CD3, CD4, and CD8 for T-cell detection and CD11b, Ly6G, and Ly6C for MDSC detection (all from BD Biosciences). Live/Dead fixable near-IR or aqua fluorescent reactive dyes (Invitrogen) were used to exclude dead cells before analysis. Cells were acquired by LSR II equipped with four lasers (BD Biosciences), and the data were analyzed with FlowJo (Tree Star).

Intracellular pH measurement

Pmel T cells were cultured at pH 7.4 in the presence of $gp100_{25\text{-}33}$ peptide for 24 hours. Cells were washed and resuspended in serum-free media and SNARF-1, acetoxymethyl ester, acetate (Life Technologies) was added to a final concentration of 10 μmol/L. After 30-minute incubation, cells were split into two aliquots that were washed two times with PBS at either pH 6.6 or 7.4. In the last wash, each of the two aliquots were again split into two aliquots at each pH and resuspended in either regular PBS at the respective pH or high-K PBS + 10 μmol/L nigericin at the respective pH. Samples were then analyzed by flow cytometry with laser excitation of approximately 543 nm and emissions at 540 and 680 nm. Ratios of fluorescence emission intensities of SNARF-1 at 580 and 640 nm, which are sensitive to pH, were then plotted.

qRT-PCR

RNA was extracted using RNeasy Isolation Kit (Qiagen). qRT-PCR was then carried out using iTaq Universal SYBR Green One-Step Kit (Bio-Rad) using the primer sequence (Table 1). Results were normalized using 36B4, then expressed as fold change (FC) = $2^{-\Delta\Delta C_t}$, where $\Delta\Delta C_t = (C_{tTarget} - C_{t36B4})assay - (C_{tTarget} - C_{t36B4})control$ (37).

Table 1. Primers and sequences

Primers	Sequence
36B4	
Forward	5′-CCGATCTGCAGACACACACT -3′
Reverse	5′-TCCAGCAGGTGTTTGACAAC -3′
IFN γ	
Forward	5′CGCTTATGTTGTTGCTGATGG-3′
Reverse	5′CACACTGCATCTTGGCTTTG-3′

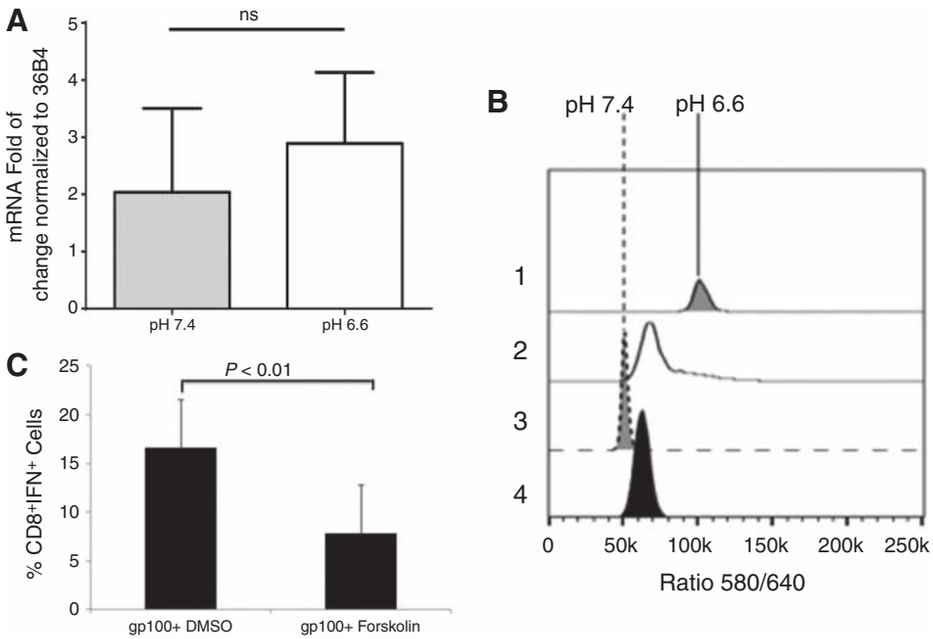

Figure 2.
T-cell characteristics. A, IFNγ mRNA levels are unaffected by pH. Levels of IFNγ mRNA in pmel T cells following a 48-hour stimulation at pH 7.4 and subsequent incubation at pH 7.4 or 6.6 for a subsequent 24 hours. Data were normalized to ribosomal protein 36B4 and expressed as mean ratio ± SD from three independent experiments; B, pHi of activated T cells is unaffected by the incubation pH. Pmel T cells were activated as above and then incubated at pH 6.6 or 7.4 for 24 hours, after which they were loaded with SNARF-1, acetoxymethyl ester, acetate, washed, and resuspended in PBS (2,4) or high K/nigericin (1,3) at pH 6.6 (1,2) or 7.4 (3,4) and the 580/640 fluorescence ratio subsequently determined by flow cytometry. The ratio shows that the pHi values of cells in PBS at low and high pH were both approximately 7.2, and the ratios in nigericin show pH calibration points. C, forskolin inhibits T-cell function. Activated pmel T cells were cultured with DMSO or forskolin in the presence of gp100 peptide. After 24 hours, intracellular IFNγ was measured by flow cytometry. Data represent results from three separate experiments, and *P* values were determined using two-tailed Student *t* test.

Statistical analyses

As indicated, unpaired Mann–Whitney or two-sided Student *t* tests were used to compare between two treatment groups. All statistical evaluations of data were performed using the GraphPad Prism Software. Statistical significance was achieved at $P < 0.05$.

Results

To investigate the effect of pH on T-cell activation *in vitro*, we used $CD8^+$ T cells isolated from pmel mice, which transgenically express a TCR specific for the melanocyte-associated peptide, $gp100_{25\text{-}33}$. These T cells were cultured with $gp100_{25\text{-}33}$ peptide for 48 hours at neutral pH and then further incubated with $gp100_{25\text{-}33}$ peptide at acidic (6.6) or alkaline (7.4) pH for an additional 24 or 48 hours. As shown in Fig. 1A, there was no significant difference in the cell viability under acidic, compared with alkaline, conditions. However, at the same time, we observed a decrease in cell-associated IFNγ (Fig. 1B). In subsequent studies, we observed that the secretion of this cytokine was completely abolished in T cells cultured under acidic conditions (Fig. 1C). The effects of acidic pH were not due to irreversible effects on $CD8^+$ signaling, as T cells, exposed to pH 6.6 for 24 hours and then shifted to pH 7.4 for 24 hours, regained the ability to secrete high levels of IFNγ (Fig. 1D). Identical results were observed when $CD8^+$ T cells isolated from OT-1 mice, which transgenically express a TCR specific for the ovalbumin peptide ($OVA_{SIINFEKL}$), were activated with $OVA_{SIINFEKL}$ peptide at low pH (Fig. 1E). We also observed a decreased secretion of TNFα by pmel and OT-I T cells cultured at pH 6.6 (data not shown). Although a similar effect was observed in T cells isolated from OT-II mice, which are $CD4^+$ T cells specific for $OVA_{323\text{–}339}$, it was not as dramatic due to a high constitutive elaboration of IFNγ from these T cells (Fig. 1F). The suppression of IFNγ was posttranscriptional, as the IFNγ mRNA levels were not significantly different in activated pmel T cells incubated at pH 6.6, compared with those at pH 7.4 (Fig. 2A). This inhibition was also not mediated by changes in the pHi. Mammalian cells in general, and immune cells in particular, have robust mechanisms that maintain a constant pHi when they are exposed to an acidic extracellular pH (pHe; ref. 38). Indeed, it has previously been shown that when lymphocytes in pHe 7.4 CM are then exposed to pHe 6.7, the pHi decreases only from 7.3 to 7.15 (33). In this study, pHi of activated T cells was measured by flow cytometry using the pH-sensitive dye, SNARF-1. The fluorescence ratios of activated T cells at pH 7.4 and 6.6 were similar, indicating that the pHi was not different, even after exposure to different pHe values (Fig. 2B). One possibility is that the effects of acidic pHe on $CD8^+$ T-cell IFNγ secretion were mediated via one or more acid-sensing receptors (34), such as ASIC3, ASIC4, OGR1, and TDAG8, which are all expressed in pmel $CD8^+$ T cells (Table 2). Evidence suggests that the effect is transduced via cAMP signaling (a TDAG8 target), as forskolin, a cAMP agonist, significantly attenuated IFNγ production, even at pH 7.4 (Fig. 2C). Also, the effect does not appear to be mediated via the PI3K pathway (an OGR1 target), as inhibition of PI3K failed to rescue IFNγ production at low pH and,

Table 2. H^+ sensors in T cells (qRT-PCR)

Receptor	Level	Second messenger
ASIC-1	+	$[Ca2^+]$
ASIC-2	–	$[Ca2^+]$
ASIC-3	++++	Na^+
ASIC-4	+++	Na^+
TRPV	–	$[Ca2^+]$
GPR4	–	cAMP
TDAG8	+++	cAMP
OGR1	++++	PI3K

indeed, led to a general inhibition at all pHs (Supplementary Fig. S1). A known function of cAMP-activated protein kinase-A is to inhibit glycolysis. We observed that activated pmel T cells at low pH had high oxygen consumption rates and low glucose-stimulated acidification rates compared with cells cultured at high pH (Fig. 3). A similar effect was observed in OT-I T cells stimulated with $OVA_{SIINFEKL}$ peptide (Supplementary Fig. S2). Unstimulated T cells are not metabolically active, and there is no effect of low pH (data not shown). This reduction of glycolysis may be consistent with the observed sequestration of *IFN*γ mRNA in cells with low glycolytic rates (39). To investigate the acid sensor, TDAG8, in more detail, T cells were isolated from TDAG8 KO or WT mice and stimulated in the presence of anti-CD3 antibodies for 48 hours at pH 6.6 or 7.4. In both TDAG8 KO and WT T cells, IFNγ production was abolished at pH 6.6 (Supplementary Fig. S3). This suggests that TDAG8 alone is not responsible for the extracellular sensing of acidity in T cells. Investigations into this and other acid-sensing receptors are ongoing to determine whether inhibition alone or in combination is effective in rescuing the phenotype at low pH.

In vivo, the acidic pHe of tumors can be increased by providing mice with 200 mmol/L *ad lib* sodium bicarbonate in drinking water (Fig. 4A). In numerous previous studies, this effect was shown to be specifically caused by buffering the pH of tumors, as it does not cause systemic alkalization nor is it due to the additional sodium load. These results were consistent with prior work in animal models where oral buffers that raise tumor pH were shown to inhibit spontaneous and experimental metastases (27, 40–42). In prior studies, bicarbonate has shown little to no effect on the growth rate of primary human tumor xenografts, neither in immunodeficient mice nor in fast-growing and aggressive B16 melanoma tumors in immunocompetent mice (28). However, in a transgenic (TRAMP) model of prostate cancer, bicarbonate therapy was shown to impair tumor development and subsequent metastases (41). In this study, as before, bicarbonate therapy had no effect on the growth rate of B16 tumors in immunocompetent C57BL/6 mice (Fig. 4B). However, there were significant ($P < 0.01$) effects of bicarbonate monotherapy on the growth of Yumm 1.1 melanoma (Fig. 4C and D). Notably, bicarbonate therapy led to significant increases in $CD8^+$ T-cell infiltrates into the Yumm 1.1 tumor (Fig. 4E). Bicarbonate monotherapy had no effect on T-cell infiltration into B16 tumors (data not shown), consistent with a lack of effect on primary tumor growth.

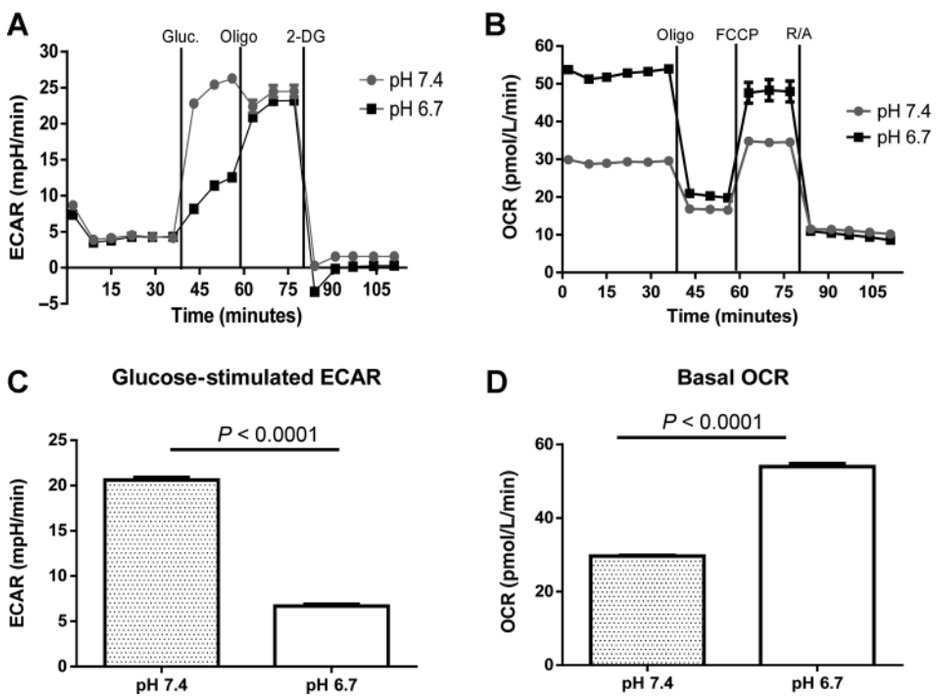

Figure 3.
pmel T-cell metabolism. Pmel T cells were activated with $gp100_{25\text{-}33}$ peptide for 48 hours, followed by a subsequent 48-hour incubation at either pH 6.7 or 7.4. Cells were subsequently metabolically profiled using a Seahorse XF-96 Analyzer. A, representative results of a glucose stress test, which measures extracellular acidification rate (ECAR) following addition of glucose (Gluc.), oligomycin (Oligo), and 2-deoxy glucose (2-DG). B, representative results of a mitochondrial stress test, which measures the oxygen consumption rate (OCR) in glucose-containing media, following sequential additions of oligomycin, FCCP, and rotenone/antimycin A. See Materials and Methods for description of glucose stress test and mitochondrial stress test. C, acidosis inhibits T-cell glycolysis. Data show the glucose-stimulated increase in ECAR. D, acidic cells are more oxidative. Data show the basal OCR for activated cells incubated at pH 6.7 or 7.4. Data represent results from three separate experiments, with six replicates per experiment. A two-tailed Student *t* test was used to calculate statistical significance.

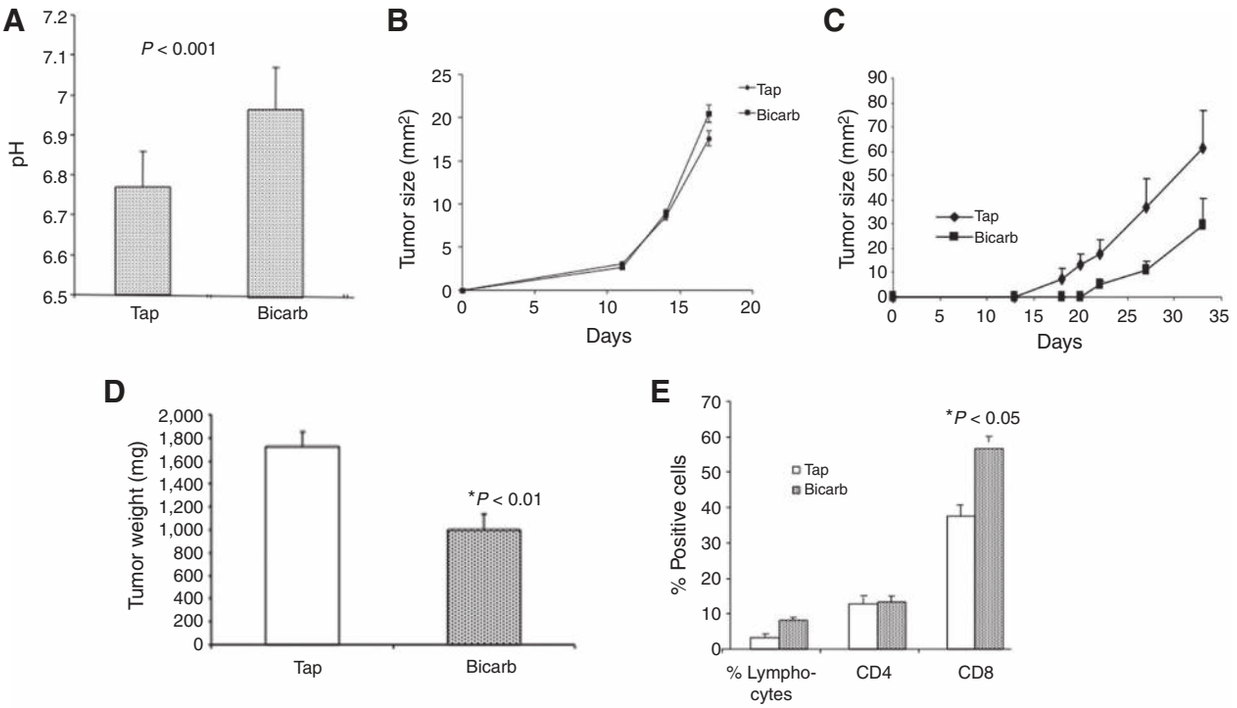

Figure 4.

Buffer monotherapy *in vivo*. Animals bearing syngeneic melanoma tumors were treated with or without 200 mmol/L *ad lib* sodium bicarbonate (Bicarb) in their drinking water. A, bicarbonate raises pHe. The pHe levels were measured with microelectrode in B16 tumors treated with or without 200 mmol/L sodium bicarbonate therapy. Four separate animals were investigated under each condition, and a minimum of four measurements were made in each tumor along a single needle track ($P < 0.001$). B, bicarbonate does not affect B16 tumor growth. Mice bearing B16 tumors were treated with or without buffer therapy, showing no effect on tumor growth ($n = 8$ mice/group). C, bicarbonate inhibits Yumm 1.1 tumor growth. Mice bearing Yumm 1.1 tumors were treated with or without buffer therapy, showing the effect on tumor growth with time ($n = 8$ mice/group). D, the resected tumor weights at the endpoint from these experiments ($P < 0.01$). E, the flow quantified relative numbers of $CD8^+$ and $CD4^+$ T-cell infiltration into Yumm 1.1 tumors ($n = 8$ mice/group; $P < 0.05$ tap vs. bicarbonate CD8 cells; CD4 not significant).

B7 and PD-L1/L2 ligands are ligands expressed by antigen-presenting cells that inhibit T-cell activation by binding to cognate checkpoint receptors CTLA4 and PD1, respectively, (43, 44), that are expressed on $CD8^+$ cytotoxic T cells. Neutralizing antibodies against CTLA4 and PD1 are being used clinically to prolong antitumor T-cell responses, and, in trials to date, response rates in melanoma range from 18% to 35% (6, 7). Given the inhibitory effect of acidosis on T cells and the reversal of acidosis with buffers, we therefore assessed if bicarbonate would augment antitumor responses in combination with anti-CTLA4 or anti-PD1 antibody therapy. We observed that combinations of bicarbonate therapy with anti-CTLA4 (Fig. 5A and B) or anti-PD1 (Fig. 5C and D) antibodies significantly improved the antitumor effects of these therapies in the B16 melanoma model that was resistant to bicarbonate alone. Although the effects on tumor growth appear modest, the morphologies of the tumors were dramatically affected by bicarbonate, in that they were macroscopically more vascularized, compared with controls (Supplementary Fig. S4). This was not a systemic effect, as there were no differences in splenic T-cell responses induced by bicarbonate in combination with PD-1 (Supplementary Fig. S4). In patients, anti-PD1 and anti-CTLA4 antibody therapies are being increasingly used in combination. When these agents were combined, there were only modest effects of adding bicarbonate therapy (Fig. 5E), likely because the combination of these checkpoint inhibitors was by itself so effective. Notably, bicarbonate in combination with either checkpoint inhibitor was as effective in suppressing tumor growth as the two-checkpoint inhibitor combination (compare Fig. 5E with 5A or 5C). Notably, the combination of bicarbonate with PD-1 checkpoint blockade was also effective in a Panc02 pancreatic cancer model. In this system, treatment with bicarbonate or anti-PD1 antibody alone had no effect on tumor growth, whereas tumors treated with combination were significantly ($P < 0.005$) smaller (Fig. 5F).

Anticancer immunotherapy also includes the adoptive cell transfer (ACT) of tumor-specific T cells. In ACT, syngeneic recipient mice bearing B16 melanomas were treated with 600 rad to deplete peripheral blood mononuclear cells, and 1 day later were infused with 10 million activated pmel (Thy1.1) T cells and subsequently treated twice a day with 250,000 IU of IL2 for 3 days. As expected, adoptive transfer alone caused significant reductions in the tumor growth rates, yet an improved antitumor response was evident, albeit not significantly, in combination with bicarbonate (Fig. 6A). However, long-term follow up showed that the combination of bicarbonate + ACT led to a long-term (censored at 120 day) survival rate of 40%, compared with 10% for ACT with pmel T cells alone (Fig. 6B). Importantly, the beneficial effects of bicarbonate were associated with

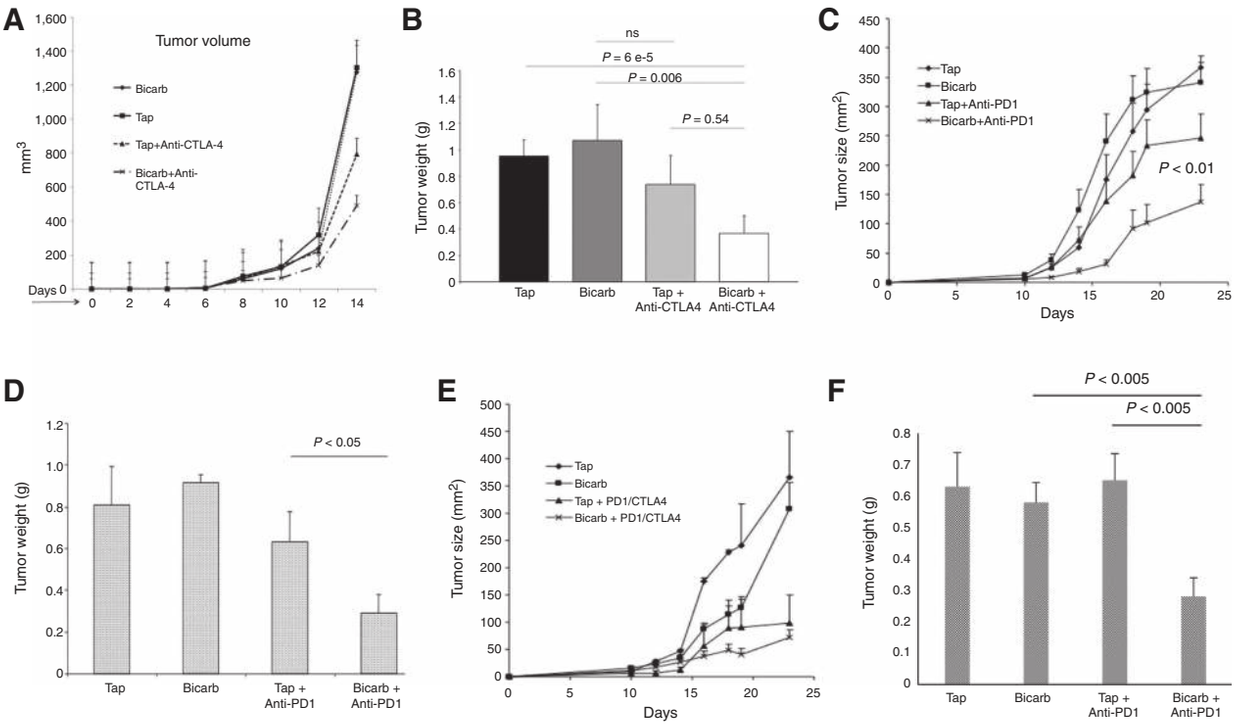

Figure 5.

Buffer therapy enhances efficacy of anti-immunotherapy in B16 melanoma. C57BL/6 mice received tap water or tap water containing 200 mmol/L sodium bicarbonate (Bicarb) *ad lib* 3 days prior to tumor inoculation with 1×10^5 tumor cells injected subcutaneously in the left flank ($n = 10$ mice/group). Three days later, animals subsequently received intraperitoneal injections of 20 mg/kg of anti-PD1 and/or anti-CTLA4 antibodies and continued to receive antibodies every 3 to 4 days until the end of the experiment. Tumor sizes were measured every 2–3 days, and at the endpoint, tumors were excised, weighed, and extracted for T-cell repertoire or prepared for histology. A and B, bicarbonate improved CTLA4 therapy in B16 melanoma. A, the growth of B16 tumors in mice treated with anti-CTLA4 antibody, with or without bicarbonate therapy. Tumor weights are shown in B. C and D, bicarbonate improved PD1 therapy in B16. C and D, the growth of B16 tumors in mice treated with anti-PD1 antibody with or without bicarbonate therapy; tumor weights are shown in D. E, bicarbonate does not add to the combination checkpoint blockade. Panel shows growth of B16 tumors in mice treated with the combination of anti-CTLA4 and anti-PD1 antibodies with or without bicarbonate therapy. Differences between checkpoint combination with or without bicarbonate were not significant. F, bicarbonate improved PD1 therapy in Panc02. Data show weights of Panc02 tumors in mice ($n = 10$ per group) treated with combination of anti-PD1 antibodies with or without bicarbonate therapy.

significant increases in T-cell persistence (Fig. 6C), a sensitive biomarker for response to adoptive T-cell therapy (45).

Discussion

In this study, we have shown that the acidic pH encountered in a tumor microenvironment has significant immunosuppressive effects. *In vitro*, acidic pH was shown to profoundly inhibit T-cell responses, including an abrogation of IFNγ and TNFα secretion, suggesting that an acidic environment may lead to a general block of translation of proinflammatory cytokines. This does not appear to be a general blockade of exocytosis, as the intracellular levels of IFNγ protein were likewise reduced and, indeed, low pH has been shown to stimulate exocytosis in a number of systems (46). An inhibition of glycolytic activation, which is necessary for T-cell activation, was also observed. Additional studies will be required to define the molecular mechanisms leading to the inhibition of glycolytic activation by acidic pH in this system. This is a significant scientific problem as acid-induced inhibition of glycolysis is known to occur in almost all systems, yet the signal transduction events are unknown. *In vivo*, treatment of mice bearing melanoma with bicarbonate therapy raised tumor pH and increased the durable response rates to both checkpoint inhibition (PD-1 and CTLA4) and adoptive cell therapy. In prior work, we have shown that buffer therapy induces "compensated metabolic alkalosis" and works by buffering the tumor pH to more neutral values, without affecting systemic pH (47).

We have calculated from these mouse studies that the human equivalent dose would be bicarbonate at 800 mg kg^{-1} d^{-1}. This dose is clinically achievable, and early-phase I clinical trials of bicarbonate therapy have been conducted. Buffer therapy directly targets the tumor pH, but there are alternative pharmacologic approaches that may indirectly lead to the same effect, i.e., compensated metabolic alkalosis, such as K-sparing diuretics (furosemide) or pan-specific carbonic anhydrase inhibitors (acetazolamide). Other approaches could target the rate of tumor acid production through either isoform-specific CAIX inhibitors (DH-348) or inhibition of LDH-A (FX-11). The ability of these agents to neutralize tumor pH is not known, nor are their effects on antitumor immunotherapy.

Harold Dvorak famously characterized tumors as "wounds that do not heal" (48). One component of the wound response is a transient ischemia–driven tissue acidification, which resolves as the wound heals (49). The role of acidification in physiologic wound healing is not known with certainty, but recent data suggest that acidification stimulates the production

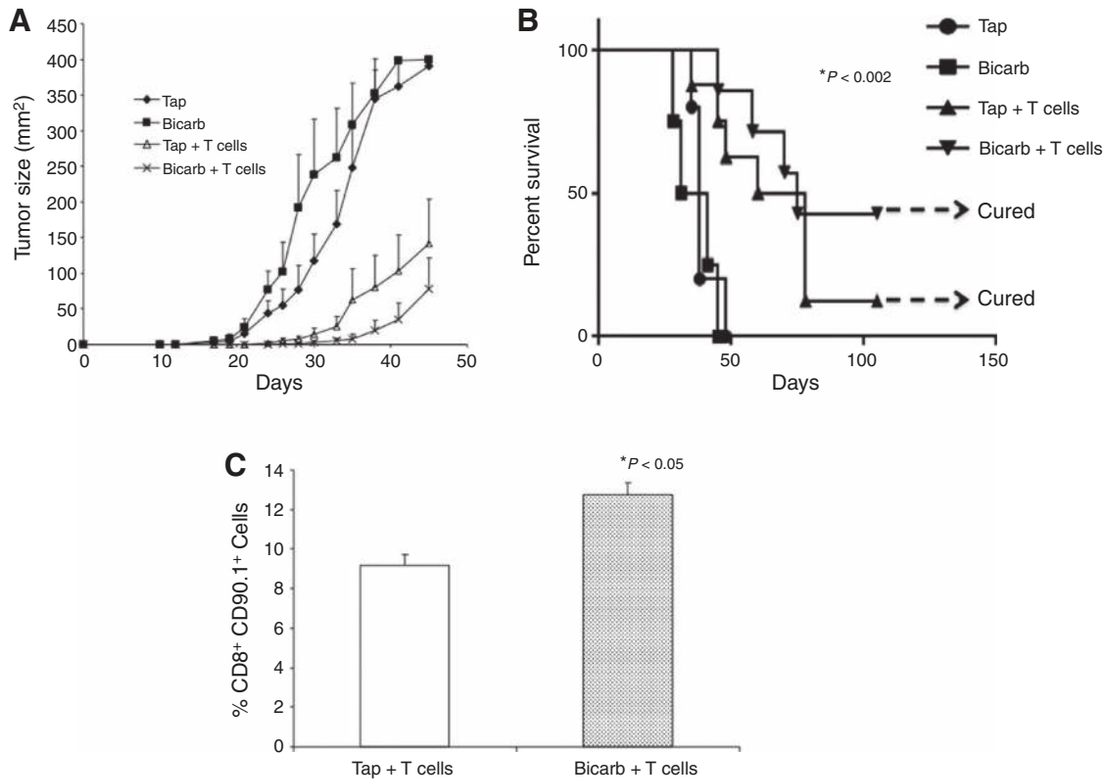

Figure 6.
Effect of bicarbonate on adoptive T-cell transfer. C57BL/6 mice ($n = 10$ per group) received tap water or tap water containing 200 mmol/L sodium bicarbonate (Bicarb) *ad lib* 3 days prior to the tumor inoculation with 1×10^5 B16 cells injected subcutaneously in the left flank. Three days after inoculation, mice received a sublethal dose (600 cGy) of TBI, administered by an X-ray irradiator. For adoptive transfer experiments, T cells were isolated from the spleens of pmel mice and cultured in media containing 10 IU/ml of IL2 and 5 μg/mL of $gp100_{25\text{-}33}$ *in vitro* for 5 days. On day 4 following tumor injection, 5×10^6 T cells were injected intravenously. IL- (2.5e5 IU) was given intraperitoneally following T-cell injection and continued every 12 hours for three days for a total of six injections. Following this treatment, tumor size was measured and recorded every 2 days. A, tumor growth after adoptive transfer of T cells or controls in combination with or without buffer therapy. Group mean differences between T cells vs. T cells + bicarbonate were not significant. However, there was a survival advantage, as shown in the survival curve in B, which had a log rank $P = 0.002$. C, percentage of T-cell persistence after adoptive transfer and buffer therapy ($P < 0.05$).

of inflammatory cytokines by the stroma or endothelium (50). As these induce neoangiogenesis, the acidosis is reduced and inflammation resolves. Our data and work cited herein would suggest that, while acidification may send an inflammatory signal, T cells are unable to activate until the pHe becomes more alkaline. In tumors, this acidification never resolves, and artificially raising the pH of tumors through buffer therapy allows the "wound" to heal by promoting antitumor immunity.

Disclosure of Potential Conflicts of Interest

R.J. Gillies has ownership interest (including patents) in and is a consultant/advisory board member for HealthMyne, Inc. No potential conflicts of interest were disclosed by the other authors.

Authors' Contributions

Conception and design: S. Pilon-Thomas, A.E. El-Kenawi, K. Luddy, M. Damaghi, J.J. Mulé, A. Ibrahim-Hashim, R.J. Gillies

Development of methodology: S. Pilon-Thomas, K.N. Kodumudi, A.E. El-Kenawi, K. Luddy, A. Ibrahim-Hashim, R.J. Gillies

Acquisition of data (provided animals, acquired and managed patients, provided facilities, etc.): S. Pilon-Thomas, A.E. El-Kenawi, S. Russell, M. Damaghi, J.W. Wojtkowiak, A. Ibrahim-Hashim, R.J. Gillies

Analysis and interpretation of data (e.g., statistical analysis, biostatistics, computational analysis): S. Pilon-Thomas, K.N. Kodumudi, A.E. El-Kenawi, S. Russell, A.M. Weber, K. Luddy, M. Damaghi, J.W. Wojtkowiak, J.M. Mulé, A. Ibrahim-Hashim, R.J. Gillies

Writing, review, and/or revision of the manuscript: S. Pilon-Thomas, K.N. Kodumudi, A.E. El-Kenawi, M. Damaghi, J.J. Mulé, A. Ibrahim-Hashim, R.J. Gillies

Administrative, technical, or material support (i.e., reporting or organizing data, constructing databases): S. Pilon-Thomas, A.M. Weber, A. Ibrahim-Hashim, R.J. Gillies

Study supervision: S. Pilon-Thomas, K.N. Kodumudi, A. Ibrahim-Hashim, R.J. Gillies

Acknowledgments

The authors thank Ms. Ellen Moore for technical assistance and Dr. Estaban Celis for early discussions of this approach.

Grant Support

This work was supported by USPHS grant R01CA077575 (R.J. Gillies), P50CA168536 (S. Pilon-Thomas), and Moffitt Cancer Center Support Grant P30CA076292.

The costs of publication of this article were defrayed in part by the payment of page charges. This article must therefore be hereby marked *advertisement* in accordance with 18 U.S.C. Section 1734 solely to indicate this fact.

Received June 30, 2015; revised November 24, 2015; accepted December 9, 2015; published OnlineFirst December 30, 2015.

References

1. Schneider H, Downey J, Smith A, Zinselmeyer BH, Rush C, Brewer JM, et al. Reversal of the TCR stop signal by CTLA-4. Science 2006;313:1972–5.
2. Vesely MD, Kershaw MH, Schreiber RD, Smyth MJ. Natural innate and adaptive immunity to cancer. Annu Rev Immunol 2011;29:235–71.
3. Hodi FS, O'Day SJ, McDermott DF, Weber RW, Sosman JA, Haanen JB, et al. Improved survival with ipilimumab in patients with metastatic melanoma. N Engl J Med 2010;363:711–23.
4. Topalian SL, Sznol M, McDermott DF, Kluger HM, Carvajal RD, Sharfman WH, et al. Survival, durable tumor remission, and long-term safety in patients with advanced melanoma receiving nivolumab. J Clin Oncol 2014;32:1020–30.
5. Taube JM, Klein A, Brahmer JR, Xu H, Pan X, Kim JH, et al. Association of PD-1, PD-1 ligands, and other features of the tumor immune microenvironment with response to anti-PD-1 therapy. Clin Cancer Res 2014;20: 5064–74.
6. Topalian SL, Hodi FS, Brahmer JR, Gettinger SN, Smith DC, McDermott DF, et al. Safety, activity, and immune correlates of anti-PD-1 antibody in cancer. N Engl J Med 2012;366:2443–54.
7. Wolchok JD, Neyns B, Linette G, Negrier S, Lutzky J, Thomas L, et al. Ipilimumab monotherapy in patients with pretreated advanced melanoma: a randomised, double-blind, multicentre, phase 2, dose-ranging study. Lancet Oncol 2010;11:155–64.
8. Fourcade J, Sun Z, Benallaoua M, Guillaume P, Luescher IF, Sander C, et al. Upregulation of Tim-3 and PD-1 expression is associated with tumor antigen-specific CD8+ T cell dysfunction in melanoma patients. J Exp Med 2010;207:2175–86.
9. Fourcade J, Sun Z, Pagliano O, Guillaume P, Luescher IF, Sander C, et al. CD8(+) T cells specific for tumor antigens can be rendered dysfunctional by the tumor microenvironment through upregulation of the inhibitory receptors BTLA and PD-1. Cancer Res 2012;72:887–96.
10. Yang ZZ, Grote DM, Ziesmer SC, Niki T, Hirashima M, Novak AJ, et al. IL-12 upregulates TIM-3 expression and induces T cell exhaustion in patients with follicular B cell non-Hodgkin lymphoma. J Clin Invest 2012;122: 1271–82.
11. Wolchok JD, Kluger H, Callahan MK, Postow MA, Rizvi NA, Lesokhin AM, et al. Nivolumab plus ipilimumab in advanced melanoma. N Engl J Med 2013;369:122–33.
12. Diaz-Montero CM, Salem ML, Nishimura MI, Garrett-Mayer E, Cole DJ, Montero AJ. Increased circulating myeloid-derived suppressor cells correlate with clinical cancer stage, metastatic tumor burden, and doxorubicin-cyclophosphamide chemotherapy. Cancer Immunol Immunother 2009; 58:49–59.
13. Pilon-Thomas S, Nelson N, Vohra N, Jerald M, Pendleton L, Szekeres K, et al. Murine pancreatic adenocarcinoma dampens SHIP-1 expression and alters MDSC homeostasis and function. PLoS One 2011;6:e27729.
14. Matsushita N, Pilon-Thomas SA, Martin LM, Riker AI. Comparative methodologies of regulatory T cell depletion in a murine melanoma model. J Immunol Methods 2008;333:167–79.
15. Peranzoni E, Zilio S, Marigo I, Dolcetti L, Zanovello P, Mandruzzato S, et al. Myeloid-derived suppressor cell heterogeneity and subset definition. Curr Opin Immunol 2010;22:238–44.
16. Nagaraj S, Gabrilovich DI. Myeloid-derived suppressor cells in human cancer. Cancer J 2010;16:348–53.
17. Kodumudi KN, Woan K, Gilvary DL, Sahakian E, Wei S, Djeu JY. A novel chemoimmunomodulating property of docetaxel: suppression of myeloid-derived suppressor cells in tumor bearers. Clin Cancer Res 2010; 16:4583–94.
18. Fallarino F, Grohmann U, Puccetti P. Indoleamine 2,3-dioxygenase: from catalyst to signaling function. Eur J Immunol 2012;42:1932–7.
19. Lardner A. The effects of extracellular pH on immune function. J Leukoc Biol 2001;69:522–30.
20. Ibrahim Hashim A, Zhang X, Wojtkowiak JW, Martinez GV, Gillies RJ. Imaging pH and metastasis. NMR Biomed 2011;24:582–91.
21. Gatenby RA, Gillies RJ. Why do cancers have high aerobic glycolysis? Nat Rev Cancer 2004;4:891–9.
22. Swietach P, Hulikova A, Vaughan-Jones RD, Harris AL. New insights into the physiological role of carbonic anhydrase IX in tumour pH regulation. Oncogene 2010;29:6509–21.
23. Choi J, Jung WH, Koo JS. Metabolism-related proteins are differentially expressed according to the molecular subtype of invasive breast cancer defined by surrogate immunohistochemistry. Pathobiology 2013;80: 41–52.
24. Ilie M, Mazure NM, Hofman V, Ammadi RE, Ortholan C, Bonnetaud C, et al. High levels of carbonic anhydrase IX in tumour tissue and plasma are biomarkers of poor prognostic in patients with non-small cell lung cancer. Br J Cancer 2010;102:1627–35.
25. Choschzick M, Oosterwijk E, Muller V, Woelber L, Simon R, Moch H, et al. Overexpression of carbonic anhydrase IX (CAIX) is an independent unfavorable prognostic marker in endometrioid ovarian cancer. Virchows Arch 2011;459:193–200.
26. Estrella V, Chen T, Lloyd M, Wojtkowiak J, Cornnell HH, Ibrahim-Hashim A, et al. Acidity generated by the tumor microenvironment drives local invasion. Cancer Res 2013;73:1524–35.
27. Ibrahim Hashim A, Cornnell HH, Coelho Ribeiro Mde L, Abrahams D, Cunningham J, Lloyd M, et al. Reduction of metastasis using a non-volatile buffer. Clin Exp Metastasis 2011;28:841–9.
28. Robey IF, Baggett BK, Kirkpatrick ND, Roe DJ, Dosescu J, Sloane BF, et al. Bicarbonate increases tumor pH and inhibits spontaneous metastases. Cancer Res 2009;69:2260–8.
29. Noritomi DT, Soriano FG, Kellum JA, Cappi SB, Biselli PJ, Liborio AB, et al. Metabolic acidosis in patients with severe sepsis and septic shock: a longitudinal quantitative study. Crit Care Med 2009;37:2733–9.
30. Calcinotto A, Filipazzi P, Grioni M, Iero M, De Milito A, Ricupito A, et al. Modulation of microenvironment acidity reverses anergy in human and murine tumor-infiltrating T lymphocytes. Cancer Res 2012; 72:2746–56.
31. Vishvakarma NK, Singh SM. Immunopotentiating effect of proton pump inhibitor pantoprazole in a lymphoma-bearing murine host: implication in antitumor activation of tumor-associated macrophages. Immunol Lett 2010;134:83–92.
32. Vishvakarma NK, Singh SM. Augmentation of myelopoiesis in a murine host bearing a T cell lymphoma following in vivo administration of proton pump inhibitor pantoprazole. Biochimie 2011;93:1786–96.
33. Bental M, Deutsch C. An NMR view of primary T-lymphocyte activation. In: Gillies RJ, editor. NMR in physiology and biomedicine. New York, NY: Academic Press; 1994.
34. Damaghi M, Wojtkowiak JW, Gillies RJ. pH sensing and regulation in cancer. Front Physiol 2013;4:370.
35. Ishii S, Kihara Y, Shimizu T. Identification of T cell death-associated gene 8 (TDAG8) as a novel acid sensing G-protein-coupled receptor. J Biol Chem 2005;280:9083–7.
36. Li Z, Dong L, Dean E, Yang LV. Acidosis decreases c-Myc oncogene expression in human lymphoma cells: a role for the proton-sensing G protein-coupled receptor TDAG8. Int J Mol Sci 2013;14: 20236–55.
37. Cougoule C, Van Goethem E, Le Cabec V, Lafouresse F, Dupre L, Mehraj V, et al. Blood leukocytes and macrophages of various phenotypes have distinct abilities to form podosomes and to migrate in 3D environments. Eur J Cell Biol 2012;91:938–49.
38. Hulikova A, Harris AL, Vaughan-Jones RD, Swietach P. Regulation of intracellular pH in cancer cell lines under normoxia and hypoxia. J Cell Physiol 2013;228:743–52.
39. Chang CH, Curtis JD, Maggi LB Jr, Faubert B, Villarino AV, O'Sullivan D, et al. Posttranscriptional control of T cell effector function by aerobic glycolysis. Cell 2013;153:1239–51.
40. Ibrahim Hashim A, Wojtkowiak JW, Ribeiro M, Estrella V, Bailey KM, Cornnell HH, et al. Free base lysine increases survival and reduces metastasis in prostate cancer model. J Cancer Sci Ther 2011;Suppl 1(4).
41. Ibrahim-Hashim A, Cornnell HH, Abrahams D, Lloyd M, Bui M, Gillies RJ, et al. Systemic buffers inhibit carcinogenesis in TRAMP mice. J Urol 2012;188:624–31.
42. Bailey KA, Wojtkowiak JW, Cornnell HH, Ribeiro MC, Balagurunathan Y, Ibrahim Hashim A, et al. Mechanisms of buffer therapy resistance. Neoplasia 2014;16:354–64.
43. Keir ME, Butte MJ, Freeman GJ, Sharpe AH. PD-1 and its ligands in tolerance and immunity. Annu Rev Immunol 2008;26:677–704.
44. McCoy KD, Le Gros G. The role of CTLA-4 in the regulation of T cell immune responses. Immunol Cell Biol 1999;77:1–10.
45. Robbins PF, Dudley ME, Wunderlich J, El-Gamil M, Li YF, Zhou J, et al. Cutting edge: persistence of transferred lymphocyte clonotypes correlates

with cancer regression in patients receiving cell transfer therapy. J Immunol 2004;173:7125–30.
46. Damaghi M, Tafreshi NK, Lloyd MC, Sprung R, Estrella V, Wojtkowiak JW, et al. Chronic acidosis in the tumour microenvironment selects for overexpression of LAMP2 in the plasma membrane. Nat Commun 2015; 6:8752.
47. Silva AS, Yunes JA, Gillies RJ, Gatenby RA. The potential role of systemic buffers in reducing intratumoral extracellular pH and acid-mediated invasion. Cancer Res 2009;69:2677–84.
48. Dvorak HF. Tumors: wounds that do not heal. Similarities between tumor stroma generation and wound healing. N Engl J Med 1986;315: 1650–9.
49. Ashby BS. pH studies in human malignant tumours. Lancet 1966;2: 312–5.
50. Dong L, Li Z, Leffler NR, Asch AS, Chi JT, Yang LV. Acidosis activation of the proton-sensing GPR4 receptor stimulates vascular endothelial cell inflammatory responses revealed by transcriptome analysis. PLoS One 2013;8: e61991.